Z. Kristallogr. **2012**, *227*, 460–467 / **DOI** 10.1524/zkri.2012.1498

Crystal structure of 2*M* and 1*A* polytypes of balangeroite

Elena Bonaccorsi*, [I], Giovanni Ferraris[II, III] and Stefano Merlino[I]

[I] Dipartimento di Scienze della Terra, Via S. Maria 53, 56126 Pisa, Italy
[II] Dipartimento di Scienze Mineralogiche e Petrologiche, Via Valperga Caluso 35, 10125 Torino, Italy
[III] Nanostructured Interfaces and Surfaces (NIS) Centre of Excellence, University of Torino

Dedicated to Friedrich Liebau for his extraordinary contributions to our understanding of the crystal chemistry of silicates

Received December 1, 2011; accepted January 19, 2012
Published online: June 25, 2012

Balangeroite / Polytypes / OD structures / (Mg,Fe) hydrate silicate / Chain silicate

Abstract. Balangeroite, with ideal crystal chemical formula $(Mg,Fe)_{42}O_6(Si_4O_{12})_4(OH)_{40}$, displays two MDO polytypes, balangeroite-2*M* ($a = 19.179$, $b = 9.601$, $c = 19.218$ Å, $\beta = 90.52°$; space group *P*2/*n*) and balangeroite-1*A* ($a = 9.602$, $b = 13.891$, $c = 14.012$ Å, $\alpha = 86.99°$, $\beta = 76.79°$, $\gamma = 76.67°$; space group $P\bar{1}$). Both polytypes are built up by octahedral walls 3×1, octahedral bundles 2×2 and four-repeat silicate chains. All these modules run parallel to the 9.6 Å axis (**b** and **a** in the monoclinic and triclinic polytype, respectively). The distinguishing features between the two polytypes are in the different positioning of the silicate chains, which gives rise to distinct cells and space groups.

Introduction

The mineral balangeroite is a magnesium and iron hydrate silicate firstly found by Compagnoni *et al.* (1983) in the serpentinites of the asbestos mine of Balangero (Turin, Italy) located in Dora-Maira massif. Its occurrence has been further investigated (Belluso and Ferraris, 1991; Groppo, 2005; Groppo *et al.*, 2006) and recently a nickel-iron analogue of balangeroite has been reported from Japan (Evans and Kuehner, 2011). Commonly balangeroite forms bundles of long brown fibres, but a prismatic variety from Balangero and other two localities (Lanzo – Ponte del Diavolo and Varisella – S. Maria della Neve) of the Dora-Maira massif were described by Groppo (2005). Due to its fibrous morphology, potential hazard of balangeroite for human health has been widely investigated (*e.g.* Groppo *et al.*, 2005).

The powder diffraction pattern clearly indicated (Compagnoni *et al.*, 1983) that balangeroite is isostructural with gageite, a fibrous manganese hydrate silicate from Franklin, New Jersey (Phillips, 1910). The disordered nature of this phase did not allow a complete structure determination, but Moore (1969) was able, through a single-crystal X-ray diffraction study, to outline a substructure ($A \sim 13.8$, $B \sim 13.7$, $C \sim 3.3$ Å, space group *Pnnm*) on the basis of the sharp and strong reflections and disregarding additional weak and diffuse reflections pointing to a triple *c* parameter. The substructure actually corresponds to the octahedral scaffolding of the mineral, consisting of two kinds of interlinked octahedral modules: 3×1 walls and 2×2 bundles, with disordered silicate tetrahedra (Moore, 1969) located in the channels running along **C**. Whereas the topology of the octahedral framework appeared to be well defined, the tetrahedral part was unknown, both as regards the number of silicate tetrahedra and as regards their actual connectedness.

A broad study on gageite and fibrous balangeroite crystals was performed by Ferraris *et al.* (1987) by means of electron diffraction and high resolution microscopy. The examination of the SAED (Selected Area Electron Diffraction) patterns and the application of the OD theory (Dornberger-Schiff, 1956; 1964; 1966; Ferraris *et al.*, 2008) allowed the authors to build a more complete structural model for both gageite and balangeroite. It includes the silicate part of the structure, which consists of four-repeat silicate single chains (*viereinfachketten*, in Liebau's terminology; Liebau, 1985) running along the 9.6 Å axis and linked to both sides of the 3×1 octahedral walls.

The structural model proposed by Ferraris *et al.* (1987) agreed with all the available experimental data, *i.e.* chemical analyses, IR spectra, and SAED patterns and pointed to the crystal chemical formula $M_{42}O_6(OH)_{40}(Si_4O_{12})_4$ (Mg and Mn dominant in the M sites in balangeroite and gageite, respectively). However, it was not possible to refine it by using X-ray diffraction data, as all the examined crystals were unsuitable for a single-crystal diffraction experiment.

In this paper we shall present the results of the refinement of the two main polytypes in prismatic samples of balangeroite from Varisella (see above), by using intensity data collected by means of a CCD-equipped Nonius Kappa diffractometer at the Department of Mineralogical and Petrological Sciences of the University of Vienna, and with a Mar CCD at the XRD1 beamline at the Elettra synchrotron radiation facility, Trieste.

* Correspondence author (e-mail: elena@dst.unipi.it)

As it was already indicated, an OD approach was very helpful in favouring the construction of the structural model. Consequently, although a detailed treatment of the OD aspects of balangeroite and gageite may be found in the original paper of Ferraris *et al.* (1987) and in Ferraris *et al.* (2008), the main results of this approach will be summarised here.

OD character of balangeroite and gageite

The X-ray and electron diffraction patterns of both balangeroite and gageite show peculiar features, such as non-space-group absences, enhancement of symmetry, and diffuseness in certain classes of reflections, features which indicate their OD character. In fact adjacent layers in both phases may follow each to the other in two geometrically equivalent ways, thus giving rise to an infinite number of possible ordered or disordered sequences (family of OD structures): the OD layers present layer symmetry $P1(1)2/m$ (the parentheses indicate the direction of missing periodicity) and translation vectors $\mathbf{a} = \mathbf{A} - \mathbf{B}$, $\mathbf{c} = 3\mathbf{C}$, and third vector (not a translation vector) $\mathbf{b}_0 = (\mathbf{A} + \mathbf{B})/2$, where **A**, **B**, **C** are the lattice vectors of the Moore's subcell. The whole set of partial operations which characterize all the possible sequences are indicated by the symbol

$$\begin{matrix} P & 1 & (1) & 2/m \\ & \{1 & (1) & 2_{2/3}/n_{1,2}\} \end{matrix}$$

where the first line gives the symmetry operations of the single layer (λ-POs) and the second line gives the operations relating adjacent layers (σ-POs; PO = partial operation). Pairs of layers related by screw operations parallel to **c** with translational component of $\pm c/3$ ($2_{\pm 2/3}$) are geometrically equivalent. An infinite number of disordered sequences as well as of polytypes (ordered sequences) may result: in the whole set pairs of adjacent layers are geometrically equivalent. It is important to stress that, in this case, only two polytypes exist which display a maximum degree of order (MDO structures in OD terminology): they are those polytypes in which not only pairs, but also triples, quadruples, ... *n*-tuples of layers are geometrically equivalent.

Polytype MDO_1 is obtained when the $2_{2/3}$ operation regularly alternates with $2_{-2/3}$: the resulting structure is monoclinic, space group symmetry $P112/n$, $\mathbf{a}_m = \mathbf{a}$, $\mathbf{b}_m = 2\mathbf{b}_0$, $\mathbf{c}_m = \mathbf{c}$; polytype MDO_2 is obtained when the $2_{2/3}$ operation is constantly applied: the resulting structure is triclinic, space group symmetry $P\bar{1}$, $\mathbf{a}_t = \mathbf{a}/2 + \mathbf{b}_0 + \mathbf{c}/3$, $\mathbf{b}_t = -\mathbf{a}/2 + \mathbf{b}_0 + \mathbf{c}/3$, $\mathbf{c}_t = \mathbf{c}$ (see Fig. 7 in Ferraris *et al.*, 1987).

Ferraris *et al.* (1987) were able to confirm the presence of both MDO polytypes among the crystals of gageite: gageite-2*M* (MDO_1) and gageite-1*A* (MDO_2), whereas only polytype MDO_1, balangeroite-2*M*, has been found among the fibrous balangeroite crystals which were the object of their investigations.

Chemical data

Quantitative electron microprobe analyses of prismatic crystals from Varisella were carried out using an ARL-SEMQ microprobe (University of Modena and Reggio Emilia, Italy) under the following operating conditions: accelerating voltage 15 kV, beam current 20 nA, beam size 20 μm; the standards used were: Amelia albite (Si), oli-

Table 1. Microprobe analyses of balangeroite crystals from Varisella.

	1	2	3	4	5	6	7	average
SiO_2	28.302	27.981	28.413	28.271	27.625	28.491	29.160	28.320
TiO_2	0.055	0.065	0.056	0.061	0.047	0.054	0.068	0.058
FeO*	19.287	19.218	19.229	19.625	19.510	19.606	19.513	19.427
Fe_2O_3	5.359	5.340	5.343	5.453	5.421	5.447	5.421	5.398
MgO	35.214	35.675	35.722	35.561	35.212	35.901	36.044	35.618
MnO	0.650	0.711	0.650	0.599	0.761	0.643	0.646	0.666
CaO	0.055	0.068	0.092	0.052	0.089	0.069	0.071	0.071
H_2O**	10.295	9.706	10.202	9.986	9.391	10.091	10.825	10.071
Atomic contents calculated on the basis of 16 silicon atoms								
Si	16.00	16.00	16.00	16.00	16.00	16.00	16.00	16.00
Ti	0.02	0.03	0.02	0.03	0.02	0.02	0.03	0.02
Fe^{2+}	9.12	9.19	9.06	9.29	9.45	9.21	8.95	9.18
Fe^{3+}	2.28	2.30	2.26	2.32	2.36	2.30	2.24	2.29
Mg	29.67	30.41	29.98	30.00	30.40	30.05	29.48	29.99
Mn	0.31	0.34	0.31	0.29	0.37	0.31	0.30	0.32
Ca	0.03	0.04	0.06	0.03	0.06	0.04	0.04	0.04
H	38.82	37.02	38.32	37.70	36.28	37.80	39.62	37.96

* The FeO and Fe_2O_3 contents have been obtained from the total Fe content assuming a Fe^{2+}/Fe^{3+} ratio of 4 : 1, as indicated by the Mössbauer study of Deriu *et al.* (1994).

** The H_2O content has been calculated assuming that the total number of anions ($O^{2-} + OH^-$) was 94, as indicated by the structural model of Ferraris *et al.* (1987).

vine (Mg), ilmenite (Fe and Ti), synthetic anorthite An_{70} (Ca), spessartine (Mn).

The FeO and Fe_2O_3 contents have been obtained from the total Fe content assuming a Fe^{2+}/Fe^{3+} ratio of 4 : 1, as indicated by the Mössbauer study of Deriu *et al.* (1994). The H_2O content has been calculated assuming that the total number of anions ($O^{2-} + OH^-$) was 94, as indicated by the structural model of Ferraris *et al.* (1987).

The analyses carried on seven distinct crystal fragments (Table 1) are largely concordant and point to the average oxide contents (wt%): SiO_2 28.320; TiO_2 0.058; FeO 19.427; Fe_2O_3 5.398; MgO 35.618; MnO 0.666; CaO 0.071; H_2O 10.071. The atomic contents have been calculated on the basis of 16 Si atoms and the resulting crystal chemical formula is:

$$(Mg_{29.99}Fe^{2+}_{9.18}Fe^{3+}_{2.29}Mn_{0.32}Ca_{0.04}Ti_{0.02})_{\Sigma 41.84} \times O_6(Si_4O_{12})_4[(OH)_{37.96}O_{2.04}]$$

Structural data and results

Monoclinic polytype

The X-ray diffraction data were collected with the same crystal of the prismatic variety of balangeroite (cross section 0.03 × 0.03 mm^2, elongation 0.20 mm) both at the XRD1 beamline of the Elettra synchrotron radiation facility at Trieste equipped with a Mar CCD, as well as through a CCD-equipped Nonius Kappa diffractometer at the Department of Mineralogical and Petrological Sciences of the University of Vienna.

As the results of the structural refinement of the two sets of data are largely concordant, we shall here discuss only those obtained with the CCD-equipped diffractometer, as they appear more precise. The unit cell orientation chosen for the data collection and structure refinement [$a = 19.179(6)$, $b = 9.601(6)$, $c = 19.218(6)$ Å, $\beta = 90.52(1)^\circ$; space group $P2/n$] presents the twofold axis along **b** and may be obtained from the orientation assumed in the paper by Ferraris *et al.* (1987) through the transformation matrix [−100/001/010].

Two different scale factors were used for the family reflections, namely those with $k = 3n$, and for the characteristic reflections, respectively (the so-called "Ďurovič effect"; Nespolo and Ferraris, 2001); a ratio of 1.7 was refined. The anisotropic refinement was carried out with SHELX (Sheldrick, 2008) starting from the atomic coordinates of the model derived on the basis of the OD theory (Ferraris *et al.*, 1987), till a final R of 0.072 for 6372 reflections with $F_o > 4\sigma(F_o)$. The occupancies of the 24 independent octahedral sites by iron and magnesium were found and refined on the basis of the scattering power of the atoms at the various sites. Details of the data collection and structure refinement are given in Table 2; the final atomic coordinates and equivalent isotropic thermal parameters are reported in Table 3. Further details of the crystal structure investigation may be obtained from crysdata@fiz-karlsruhe.de, on quoting the CSD number 424104. The tables with the selected bond distances and

Table 2. Crystal data and structure refinement for balangeroite-2*M* and balangeroite-1*A*.

	balangeroite-2*M*	balangeroite-1*A*
Wavelength	0.71073 Å	0.71073 Å
Crystal system	monoclinic	triclinic
Space group	$P2/n$	$P\bar{1}$
Unit cell dimensions	$a = 19.179$ Å $b = 9.601$ Å $c = 19.218$ Å $\beta = 90.52^\circ$	$a = 9.602$ Å $b = 13.891$ Å $c = 14.012$ Å $\alpha = 86.99^\circ$ $\beta = 76.79^\circ$ $\gamma = 76.67^\circ$
Volume	3538.6 Å^3	1770.5 Å^3
Density (calculated)	2.856 g/cm^3	3.351 g/cm^3
Crystal size	0.03 × 0.03 × 0.20 mm^3	0.05 × 0.06 × 0.20 mm^3
θ range for data collection	3.67 to 30.49°	3.42 to 30.48°
Index ranges	$-27 \le h \le 27$ $0 \le k \le 13$ $0 \le l \le 27$	$-13 \le h \le 13$ $-19 \le k \le 19$ $0 \le l \le 19$
Reflections collected	10787	10722
Completeness	99.7%	99.4%
Refinement method	Full-matrix least-squares on F^2	
Data/restraints/parameters	10787/0/693	10722/0/302
Goodness of fit	0.990	1.036
R indices $[I > 2\sigma(I)]$	$R1 = 0.0728$ $wR2 = 0.1403$	$R1 = 0.1011$ $wR2 = 0.2240$
R indices (all data)	$R1 = 0.1095$ $wR2 = 0.1548$	$R1 = 0.2495$ $wR2 = 0.2829$
Extinction coefficient	0.00016(3)	–
Largest diff. peak and hole	2.557 and −1.413 e.Å^{-3}	4.832 and −2.212 e.Å^{-3}

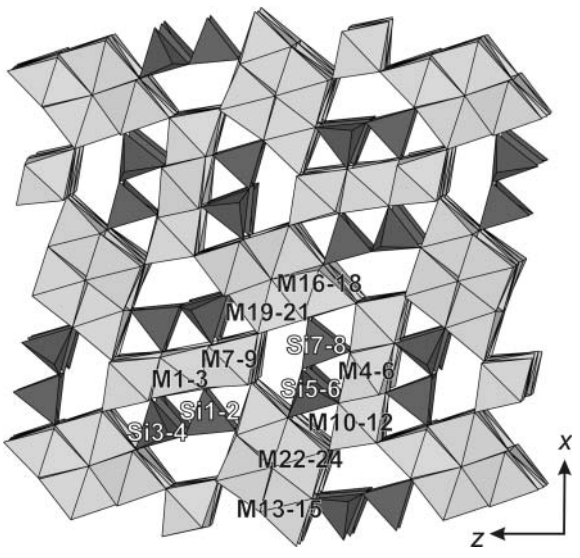

Fig. 1. Structure of balangeroite-2*M* as seen down **b**. The labels indicate the octahedral and tetrahedral sites (for example M1–3 indicates the column of M1, M2 and M3 sites.

Table 3. Final positions and equivalent isotropic thermal parameters for atoms in balangeroite-2*M*.

Site	*x*	*y*	*z*	*U*	Site	*x*	*y*	*z*	*U*
M1	0.25	0.9993(4)	0.75	0.003(1)	O9	0.0020(3)	0.1662(6)	0.0070(2)	0.010(1)
M2	0.25	0.3333(4)	0.75	0.009(1)	O10	0	0.5	0	0.011(1)
M3	0.25	0.6679(4)	0.75	0.004(1)	O11	0	0	0.5	0.010(1)
M4	0.25	0.1662(4)	0.25	0.007(1)	O12	0.0013(3)	0.3346(6)	0.5023(3)	0.011(1)
M5	0.25	0.5017(4)	0.25	0.003(1)	OH13	0.0311(2)	0.3308(6)	0.8760(3)	0.010(1)
M6	0.25	0.8310(4)	0.25	0.005(1)	O14	0.0409(2)	0.6529(6)	0.8710(2)	0.009(1)
M7	0.2275(1)	0.1664(3)	0.8899(1)	0.006(1)	OH15	0.1244(3)	0.1648(7)	0.4675(3)	0.012(1)
M8	0.2276(1)	0.5003(3)	0.8888(1)	0.006(1)	O16	0.1291(2)	0.8393(6)	0.4599(2)	0.008(1)
M9	0.2275(1)	0.8335(3)	0.8888(1)	0.004(1)	O17	0.2992(2)	0.1632(6)	0.8062(2)	0.005(1)
M10	0.1113(1)	0.9992(3)	0.2729(1)	0.005(1)	OH18	0.2085(2)	0.8333(7)	0.6958(2)	0.010(1)
M11	0.1110(1)	0.3343(3)	0.2725(1)	0.005(1)	O19	0.1943(2)	0.3387(6)	0.2001(2)	0.006(1)
M12	0.1101(1)	0.6667(3)	0.2734(1)	0.004(1)	OH20	0.1944(2)	0.6676(6)	0.2102(2)	0.007(1)
M13	0.1133(1)	0.9989(3)	0.5363(1)	0.004(1)	O21	0.1764(2)	0.6623(6)	0.8301(2)	0.006(1)
M14	0.1105(1)	0.3332(2)	0.5353(1)	0.006(1)	OH22	0.1870(2)	0.3330(7)	0.8326(2)	0.010(1)
M15	0.1136(1)	0.6674(2)	0.5349(1)	0.012(1)	O23	0.1696(2)	0.8379(6)	0.3241(2)	0.008(1)
M16	0.0344(1)	0.1668(1)	0.1103(1)	0.010(1)	OH24	0.1677(2)	0.1670(7)	0.3134(2)	0.010(1)
M17	0.0371(1)	0.5020(3)	0.1135(1)	0.004(1)	OH25	0.0825(3)	0.8321(7)	0.5974(2)	0.011(1)
M18	0.0386(1)	0.8315(3)	0.1173(1)	0.008(1)	O26	0.0885(2)	0.1579(7)	0.6073(2)	0.010(1)
M19	0.0757(1)	0.0016(2)	0.9763(1)	0.008(1)	OH27	0.1013(3)	0.6699(6)	0.0826(3)	0.010(1)
M20	0.0764(1)	0.3352(2)	0.9758(1)	0.008(1)	O28	0.1063(3)	0.3457(6)	0.0888(3)	0.011(1)
M21	0.0745(1)	0.6628(2)	0.9751(1)	0.008(1)	O29	0.0394(3)	0.0156(6)	0.8713(3)	0.008(1)
M22	0.0259(1)	0.1647(2)	0.4245(1)	0.007(1)	O30	0.1284(3)	0.4960(7)	0.4608(3)	0.011(1)
M23	0.0234(1)	0.4977(2)	0.4241(1)	0.007(1)	OH31	0.2798(3)	0.9990(6)	0.9376(2)	0.009(1)
M24	0.0233(1)	0.8367(2)	0.4241(1)	0.008(1)	OH32	0.2800(2)	0.6672(6)	0.9365(2)	0.008(1)
Si1	0.1183(1)	0.1768(2)	0.6845(1)	0.005(1)	OH33	0.2834(2)	0.3331(6)	0.9376(2)	0.009(1)
Si2	0.1184(1)	0.4877(2)	0.6839(1)	0.007(1)	OH34	0.0635(2)	0.1663(7)	0.2158(2)	0.010(1)
Si3	0.0956(1)	0.6760(2)	0.8094(1)	0.005(1)	OH35	0.0623(2)	0.5011(6)	0.2204(2)	0.008(1)
Si4	0.0957(1)	0.9888(2)	0.8101(1)	0.008(1)	OH36	0.0621(2)	0.8321(7)	0.2212(2)	0.009(1)
Si5	0.1912(1)	0.8234(2)	0.4044(1)	0.005(1)	O37	0.2985(2)	0.5040(6)	0.8056(2)	0.008(1)
Si6	0.1906(1)	0.5137(2)	0.4043(1)	0.008(1)	O38	0.1946(2)	0.9944(6)	0.2019(2)	0.008(1)
Si7	0.1838(1)	0.0116(2)	0.1185(1)	0.008(1)	O39	0.1774(2)	0.0055(6)	0.8307(3)	0.008(1)
Si8	0.1842(1)	0.3244(2)	0.1185(1)	0.004(1)	O40	0.1692(2)	0.4954(6)	0.3230(2)	0.008(1)
O1	0.0764(3)	0.5861(6)	0.7397(3)	0.012(1)	OH41	0.1468(2)	0.1685(7)	0.9611(2)	0.009(1)
O2	0.2251(2)	0.6674(6)	0.4170(2)	0.010(1)	OH42	0.1479(3)	0.4995(7)	0.9604(2)	0.010(1)
O3	0.0822(2)	0.8345(6)	0.7775(2)	0.010(1)	OH43	0.1448(2)	0.8319(7)	0.9580(2)	0.010(1)
O4	0.0937(2)	0.3341(6)	0.7102(2)	0.011(1)	OH44	0.0391(3)	0.0033(6)	0.3525(3)	0.009(1)
O5	0.2594(3)	0.9161(6)	0.4244(3)	0.011(1)	OH45	0.0392(2)	0.3310(6)	0.3529(2)	0.009(1)
O6	0.2413(3)	0.4156(6)	0.0759(3)	0.011(1)	OH46	0.0410(2)	0.6678(6)	0.3553(2)	0.010(1)
O7	0.0765(3)	0.0823(6)	0.7404(3)	0.010(1)	O47	0.0886(3)	0.5095(6)	0.6048(3)	0.009(1)
O8	0.2087(2)	0.1668(6)	0.0953(2)	0.010(1)	O48	0.1053(2)	0.9852(6)	0.0883(3)	0.007(1)

the list of F_o–F_c may be obtained from the authors upon request.

The crystal structure is illustrated in Figs. 1 and 2, which describe the connection between the various polyhedral modules.

Octahedral modules. The octahedral scaffolding is built up with two distinct modules, namely 3 × 1 walls of octahedra (sites M1–M12; two crystallographically independent walls run in the unit cell, parallel to **b**, with the M sites of the central column of each one placed along a twofold axis) and 2 × 2 bundles of octahedra (sites M13–M24); also in this case two crystallographically independent modules run parallel to **b**, which is also the direction of elongation of the crystal. The two types of modules are interlinked through corner sharing. Table 4 presents the occupancies and the average bond distances M–O for each octahedral site.

The data of Table 4 show that the iron substitution occurs mainly in the bundles, where all the sites present mixed occupancy by Mg and Fe, with the exception of M16 and M18 which are fully occupied by Fe and Mg, respectively; the last site presents a peculiar coordination with five short distances (2.03 to 2.11 Å) to the corners of

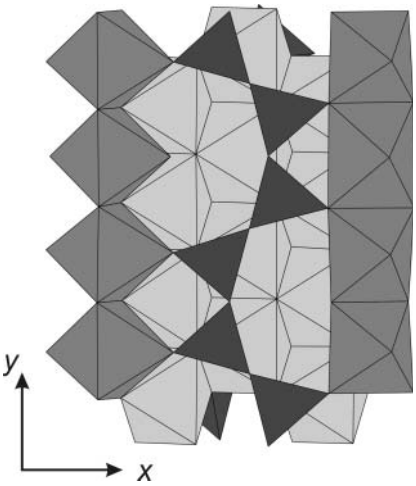

Fig. 2. The connection of the tetrahedral chains with the octahedral framework in balangeroite-2*M* as seen down **c**. The chains are attached to both sides of the walls (light grey octahedra) and are laterally connected to the bundles (dark grey octahedra).

a tetragonal pyramid, and a longer distance (2.51 Å) to complete a 'pseudo-octahedral' coordination. It is evident a correlation between the Fe content and the average bond distance. It is proper to observe that, whereas the average bond distances observed in the octahedra of the walls agree well with the values calculated from the ionic radii, those observed in the bundles are systematically and significantly larger than the calculated ones. This bond elongation has been observed also in the bundles which characterize the crystal structure of wightmanite (Moore and Araki, 1974) and may be explained with the relatively strong cation-cation repulsions which occur in the bundles. These repulsions cannot be released through the normal shortening of the shared edges parallel to the 'fibre' axis, because such shortening would produce an untenable misfit between the bundles and the other polyhedral modules of the structure.

Tetrahedral module. The channels of the octahedral framework are occupied by four-repeat silicate chains which are placed on both sides of the octahedral walls, and are related by the twofold axis running along the central column of the walls (Fig. 1). They are also laterally connected with the octahedral bundles, as it is shown in Fig. 2. This kind of chain has been found in various other minerals. In balangeroite the chain is particularly extended, as it is shown in Table 5, which compares the repeat period and corresponding Si···Si···Si angle in some phases characterised by the presence of four-repeat silicate chains. The examination of the angles reported in Table 5 indicates that the four-repeat chain is extremely flexible, adapting itself to quite different structural modules. In balangeroite, the chain has to match the size of three edge sharing octahedra, giving rise to a periodicity of 9.601 Å, significantly longer than that of the other phases in the table.

Table 4. Occupancies and average M−O bond distances (Å) for the octahedral sites in balangeroite-2*M*.

Site	Occupancy	⟨M−O⟩	Site	Occupancy	⟨M−O⟩
M1	Mg	2.093	M13	$Mg_{0.95}Fe_{0.05}$	2.132
M2	$Mg_{0.82}Fe_{0.18}$	2.111	M14	$Mg_{0.56}Fe_{0.44}$	2.157
M3	Mg	2.089	M15	$Mg_{0.61}Fe_{0.39}$	2.165
M4	$Mg_{0.84}Fe_{0.16}$	2.119	M16	Fe	2.206
M5	Mg	2.093	M17	$Mg_{0.95}Fe_{0.05}$	2.131
M6	Mg	2.085	M18	Mg	2.138
M7	Mg	2.110	M19	$Mg_{0.34}Fe_{0.66}$	2.174
M8	Mg	2.108	M20	$Mg_{0.43}Fe_{0.57}$	2.171
M9	Mg	2.123	M21	$Mg_{0.55}Fe_{0.45}$	2.149
M10	Mg	2.111	M22	$Mg_{0.79}Fe_{0.21}$	2.143
M11	Mg	2.114	M23	$Mg_{0.36}Fe_{0.64}$	2.169
M12	Mg	2.118	M24	$Mg_{0.28}Fe_{0.72}$	2.171

Table 5. Repeat period and Si...Si...Si angle in minerals characterized by Si_4O_{12} four-repeat silicate chain.

Phase	Period (Å)	Angle (°)	Reference
Haradaite	7.031	96.1	a, b
$BaUO_2Si_2O_6$	7.496	101.1	c
Fukalite	7.573	101.0	d
Ohmilite	7.799	104.1	e
Batisite	8.140	106.6	f
Balangeroite-2*M*	9.601	126.6	this work

(a) Takéuchi and Joswig, 1967; (b) Basso *et al.*, 1995; (c) Plaisier *et al.*, 1995; (d) Merlino *et al.*, 2009; (e) Mizota *et al.*, 1983; (f) Rastvetaeva *et al.*, 1997.

Bond valence balance and hydrogen bond system. The examination of the bonding environment of the various anionic sites allows one to easily distinguish the O^{2-} and OH^- anions: among the 48 independent anionic sites (46 in general position and 2 in special position on inversion centres), 24 correspond to oxide anions: 8 are linked to two Si cations (bridging atoms); 16 are linked to one Si and three M cations; 4 (two of them in special position on inversion centres) are placed along the central rows of the octahedral bundles and are linked to six M cations. The remaining 20 anionic sites are linked to three M cations only and obviously correspond to hydroxyl anions. The bond valence calculations (Brese and O'Keeffe, 1991) confirm these indications, giving bond valence sums between 1.87 and 2.00 *v.u.* for the oxide anions linked to silicon atoms and between 0.96 and 1.18 *v.u.* for the hydroxyl anions. The exceptions are represented by the four oxide anions linked to six M cations in the octahedral bundles, with bond valence sums between 1.49 and 1.58 *v.u.*; a similar undersaturation is shown by the oxide anions located in the central rows of the octahedral bundles which occur in the structure of wightmanite. As in that case, the undersaturation appears as an artefact of the bond valence calculations, dependent on the abnormal bond elongation which has been observed in the octahedral bundles of both structure types.

Each of the eight bridging oxygen atoms in the silicate chains is acceptor in two hydrogen bonds of medium strength (O···O distances between 2.80 and 2.95 Å, with only one distance of 3.01 Å) from hydroxyl anions. The remaining four OH^- anions are donors in four weak hy-

drogen bonds (O···O distances between 3.02 and 3.11 Å) to four hydroxyl anions, which are, consequently, both acceptor and donor.

Triclinic polytype

As already said, Ferraris *et al.* (1987) in their electron diffraction study did not find evidence for the presence of the triclinic MDO polytype of balangeroite. Its actual presence in the sample of prismatic balangeroite from Varisella here studied has been confirmed and a full set of X-ray diffraction data were collected by the mentioned CCD-equipped Nonius Kappa diffractometer, with a crystal presenting the following dimensions: cross section 0.06 × 0.05 mm^2, elongation 0.20 mm. The starting atomic coordinates have been assessed on the basis of the model derived through the application of the OD theory, and the isotropic refinement has been carried out following the same procedures we have used in the study of the monoclinic polytype [final $R = 0.102$ for 4424 reflections with $F_o > 4\sigma(F_o)$]. Details of the data collection and structure refinement are included in Table 2; the final atomic coordinates and isotropic thermal parameters are given in Table 6, whereas further details of the crystal structure investigation may be obtained from crysdata@fiz-karlsruhe.de, on quoting the CSD number 424105. The tables with the selected bond distances and the list of F_o–F_c may be obtained from the authors upon request.

Table 6. Final positions and isotropic thermal parameters for atoms in balangeroite-1*A*.

Site	*x*	*y*	*z*	*U*	Site	*x*	*y*	*z*	*U*
M1	0.1650(5)	0.9997(4)	0.4997(4)	0.010(1)	O10	0.0	0.0	0.0	0.011(3)
M3	0.50	0.0	0.5	0.002(1)	O11	0.0	0.5	0.5	0.010(3)
M4	0.0	0.5	0.0	0.014(1)	O12	0.3387(11)	0.4928(7)	0.4957(7)	0.004(2)
M5	0.6664(5)	0.5004(4)	0.0000(4)	0.013(1)	O13	0.3119(12)	0.9098(8)	0.1674(8)	0.012(2)
M7	0.0153(4)	0.1176(3)	0.3372(3)	0.002(1)	OH14	0.6430(11)	0.9085(8)	0.1606(8)	0.008(2)
M8	0.3471(5)	0.1163(3)	0.3386(3)	0.008(1)	OH15	0.0851(10)	0.5929(7)	0.6571(7)	0.005(2)
M9	0.6833(5)	0.1153(3)	0.3385(4)	0.018(1)	O16	0.7580(10)	0.5890(7)	0.6690(7)	0.004(2)
M10	0.9265(5)	0.3830(3)	0.8387(3)	0.010(1)	OH17	0.9704(10)	0.0987(7)	0.4867(7)	0.003(2)
M11	0.2594(5)	0.3837(3)	0.8376(4)	0.019(1)	O18	0.7036(11)	0.8973(7)	0.5084(8)	0.006(2)
M12	0.5928(4)	0.3836(3)	0.8379(3)	0.002(1)	O19	0.2069(11)	0.3958(7)	0.9920(7)	0.005(2)
M13	0.9263(4)	0.6499(3)	0.5766(3)	0.011(1)	OH20	0.5371(11)	0.4031(7)	0.9875(7)	0.006(2)
M14	0.2544(5)	0.6533(3)	0.5777(3)	0.037(1)	OH21	0.5443(10)	0.0171(7)	0.3525(7)	0.004(2)
M15	0.5925(2)	0.6451(2)	0.5764(2)	0.005(1)	O22	0.2202(11)	0.0081(8)	0.3457(8)	0.007(2)
M16	0.1437(3)	0.1461(2)	0.9246(2)	0.005(1)	O23	0.7238(10)	0.4949(7)	0.8475(7)	0.004(2)
M17	0.4759(4)	0.1502(3)	0.9224(3)	0.017(1)	OH24	0.0544(10)	0.4810(7)	0.8522(7)	0.004(2)
M18	0.8088(4)	0.1492(3)	0.9221(3)	0.007(1)	O25	0.7827(11)	0.6940(8)	0.4821(8)	0.009(2)
M19	0.9477(3)	0.0522(2)	0.0994(2)	0.008(1)	OH26	0.1156(10)	0.6842(7)	0.4827(7)	0.004(2)
M20	0.2855(3)	0.0521(2)	0.0992(2)	0.002(1)	OH27	0.5991(11)	0.1835(7)	0.0168(7)	0.007(2)
M21	0.6150(4)	0.0498(3)	0.1009(3)	0.015(1)	O28	0.2703(10)	0.1953(7)	0.0180(7)	0.007(2)
M22	0.1490(3)	0.4481(2)	0.6005(2)	0.006(1)	O29	0.9705(11)	0.9105(8)	0.1661(8)	0.008(2)
M23	0.4829(3)	0.4481(2)	0.5993(2)	0.007(1)	O30	0.4018(10)	0.5890(7)	0.6685(7)	0.006(2)
M24	0.8201(3)	0.4494(2)	0.5996(2)	0.013(1)	OH31	0.8156(11)	0.2164(7)	0.3416(8)	0.005(2)
Si1	0.7455(4)	0.8026(2)	0.4347(2)	0.000(1)	OH32	0.4785(11)	0.2201(7)	0.3468(7)	0.006(2)
Si2	0.4316(4)	0.8025(3)	0.4341(3)	0.005(1)	OH33	0.1441(10)	0.2185(7)	0.3430(7)	0.002(2)
Si3	0.2600(4)	0.9050(3)	0.2865(3)	0.001(1)	OH34	0.1255(11)	0.2790(7)	0.8462(8)	0.006(2)
Si4	0.9482(4)	0.9049(3)	0.2860(3)	0.005(1)	OH35	0.4584(10)	0.2828(7)	0.8428(7)	0.003(2)
Si5	0.6963(4)	0.5951(2)	0.7859(3)	0.001(1)	OH36	0.7906(10)	0.2835(7)	0.8426(7)	0.003(2)
Si6	0.3835(4)	0.5948(3)	0.7863(3)	0.003(1)	O37	0.3590(10)	0.8966(7)	0.5061(7)	0.003(2)
Si7	0.8873(4)	0.3023(3)	0.0650(3)	0.004(1)	O38	0.8669(10)	0.3963(7)	0.9920(7)	0.004(2)
Si8	0.2015(4)	0.3030(3)	0.0661(3)	0.001(1)	O39	0.8766(10)	0.0072(7)	0.3475(7)	0.004(2)
O1	0.6048(9)	0.8042(6)	0.3855(6)	0.009(2)	O40	0.3827(10)	0.4920(7)	0.8471(7)	0.004(2)
O2	0.5188(9)	0.6406(6)	0.8049(6)	0.007(2)	OH41	0.0717(11)	0.1038(8)	0.1867(8)	0.006(2)
O3	0.8675(9)	0.8164(6)	0.3347(6)	0.008(2)	OH42	0.4040(11)	0.1072(7)	0.1878(7)	0.005(2)
O4	0.3642(9)	0.8162(6)	0.3360(6)	0.007(2)	OH43	0.7323(10)	0.1073(7)	0.1853(7)	0.003(2)
O5	0.7431(9)	0.6830(6)	0.8365(6)	0.009(2)	OH44	0.9736(11)	0.3912(7)	0.6863(7)	0.003(2)
O6	0.2445(9)	0.6833(6)	0.8361(6)	0.007(2)	OH45	0.3045(11)	0.3926(7)	0.6867(8)	0.007(2)
O7	0.1117(9)	0.8579(6)	0.3056(6)	0.008(2)	OH46	0.6411(10)	0.3971(7)	0.6860(7)	0.004(2)
O8	0.0264(9)	0.3037(6)	0.1158(6)	0.005(2)	O47	0.4283(10)	0.6929(7)	0.4830(7)	0.006(2)
O9	0.1669(12)	0.0041(8)	0.9985(9)	0.007(2)	O48	0.9228(11)	0.1912(8)	0.0173(8)	0.008(2)

The unit cell orientation chosen for the data collection and structure refinement [$a = 9.602(6)$, $b = 13.891(6)$, $c = 14.012(6)$ Å, $\alpha = 86.99(1)°$, $\beta = 76.79(1)°$, $\gamma = 76.67(1)°$; space group $P\bar{1}$] corresponds to that of the reduced cell and may be obtained from the orientation assumed in the paper by Ferraris *et al.* (1987) through the transformation matrix [001/010/100]. With the present orientation, the octahedral walls and bundles – as well as the tetrahedral chains – run along **a**, which is also the direction of elongation of the crystal.

The distinguishing features between balangeroite-2*M* and balangeroite-1*A* lie in the different relative positioning of the silicate chains sandwiching the octahedral walls, which gives rise to distinct cells and space group symmetries [see Fig. 7a, b in Ferraris *et al.* (1987)].

Conclusions

Our structural refinements fully confirm the results obtained through electron diffraction (Ferraris *et al.*, 1987): the polytypic nature of balangeroite, the structural models derived on the basis of the OD approach, the structural relationships between the two MDO polytypes. Moreover they allow an appraisal of the details of the structural arrangements and an appreciation of the distinguishing features between the monoclinic and the triclinic polytype.

The results of the refinement carried out for balangeroite-1*A* point to a higher iron content (18.68 Fe atoms in the unit formula, to compare with 10.70 for balangeroite-2*M*; Table 7). Unfortunately, the measured triclinic crystal of balangeroite is the only one we have so far found and we could not obtain a WDS chemical analysis of it; in fact, its small dimensions resulted unsuitable for preparing a polished section.

We note that the plot reported in Fig. 3.20 of Groppo (2005) shows a wide spread of iron content for the prismatic form of balangeroite; the spread is by far more limited in the fibrous form. According to Groppo (2005), the fibrous balangeroite variety is formed at the expenses of the pre-existent prismatic balangeroite. Clearly, during the prismatic to fibrous transformation, the different variable content of iron in the mother prismatic material was averaged. The absence of triclinic balangeroite in the fibrous samples studied by Ferraris *et al.* (1987) could support the hypothesis that conditions favourable to the formation of triclinic balangeroite were realized only at higher concentration of iron.

Table 7. Occupancies and average M–O bond distances (Å) for the octahedral sites in balangeroite-1*A*.

Site	Occupancy	⟨M–O⟩	Site	Occupancy	⟨M–O⟩
M1	$Mg_{0.81}Fe_{0.19}$	2.089	M14	$Mg_{0.43}Fe_{0.57}$	2.136
M3	$Mg_{0.82}Fe_{0.18}$	2.121	M15	$Mg_{0.05}Fe_{0.95}$	2.196
M4	$Mg_{0.60}Fe_{0.40}$	2.115	M16	$Mg_{0.49}Fe_{0.51}$	2.150
M5	$Mg_{0.72}Fe_{0.28}$	2.089	M17	$Mg_{0.54}Fe_{0.46}$	2.138
M7	$Mg_{0.89}Fe_{0.11}$	2.121	M18	$Mg_{0.61}Fe_{0.39}$	2.172
M8	$Mg_{0.86}Fe_{0.14}$	2.110	M19	$Mg_{0.18}Fe_{0.82}$	2.170
M9	$Mg_{0.75}Fe_{0.25}$	2.115	M20	$Mg_{0.28}Fe_{0.72}$	2.173
M10	$Mg_{0.80}Fe_{0.20}$	2.110	M21	$Mg_{0.44}Fe_{0.56}$	2.143
M11	$Mg_{0.73}Fe_{0.27}$	2.108	M22	$Mg_{0.35}Fe_{0.65}$	2.171
M12	$Mg_{0.90}Fe_{0.10}$	2.128	M23	$Mg_{0.18}Fe_{0.82}$	2.171
M13	$Mg_{0.64}Fe_{0.36}$	2.135	M24	$Mg_{0.30}Fe_{0.70}$	2.149

Acknowledgements. The authors thank Dr. Chiara Groppo, who kindly provided the sample of prismatic balangeroite, Dr. Angela Gula, who collected the data at Vienna, and Dr. Francesco Vincentini, who helped in the structure refinements. The constructive suggestions of Prof. Emil Makovicky and two anonymous referees greatly improved the readability of the paper, and we are grateful to all them. This work was supported by MIUR (Ministero dell'Istruzione, dell'Università e della Ricerca) through grants to the national project PRIN 2009 'Structures, microstructures and properties of minerals'.

References

Basso, R.; Lucchetti, G.; Palenzona, A.; Zefiro, L.: Haradaite from the Gambatesa mine, eastern liguria. Neues Jahrbuch für Mineralogie, Monatshefte (1995) 281–288.

Belluso, E.; Ferraris, G.: New data on balangeroite and carlosturanite from alpine serpentinites. Eur. J. Mineral. **3** (1991) 559–566.

Brese, N. E.; O'Keeffe, M.: Bond-valence parameters for solids. Acta Crystallogr. **B47** (1991) 192–197.

Compagnoni, R.; Ferraris, G.; Fiora, L.: Balangeroite, a new fibrous silicate related to gageite from Balangero, Italy. Am. Mineral. **68** (1983) 214–219.

Deriu, A.; Ferraris, G.; Belluso, E.: ^{57}Fe Mössbauer study of the asbestiform silicates balangeroite and carlosturanite. Phys. Chem. Minerals **21** (1994) 222–227.

Dornberger-Schiff, K.: On the order-disorder (OD-structures). Acta Crystallogr. **9** (1956) 593–601.

Dornberger-Schiff, K.: Grundzüge einer Theorie von OD-Strukturen aus Schichten. Abhandlungen der Deutschen Akademie der Wissenschaften zu Berlin, Klasse für Chemie, Geologie und Biologie **3** (1964) 1–107.

Dornberger-Schiff, K.: Lehrgang über OD-Strukturen. Akademie-Verlag, Berlin 1966.

Evans, B. W.; Kuehner, S. M.: A nickel-iron analogue of balangeroite and gageite (Sasaguri, Kyushu, Japan). Eur. J. Mineral. **23** (2011) 717–720.

Ferraris, G.; Makovicky E.; Merlino S.: Crystallography of modular materials. IUCr Monographs on Crystallography 15, Oxford University Press, New York, 2008.

Ferraris, G.; Mellini, M.; Merlino, S.: Electro-diffraction and electron-microscopy study of balangeroite and gageite: crystal structures, polytypism and fiber textures. Am. Mineral. **72** (1987) 382–391.

Groppo, C.: Rischio amianto nelle Alpi Occidentali. PhD Thesis, University of Turin, Italy, 2005.

Groppo, C.; Rinaudo, C.; Cairo, S.; Gastaldi, D.; Compagnoni, R.: Micro-Raman spectroscopy for a quick and reliable identification of serpentine minerals from ultramafics. Eur. J. Mineral. **18** (2006) 319–329.

Groppo, C.; Tomatis, M.; Turci, F.; Gazzano, E.; Ghigo, D.; Compagnoni, R.; Fubini, B.: Potential toxicity of nonregulated asbestiform minerals: balangeroite from western Alps. Part 1: Identification and characterization. J. Toxicol. Environ. Health, Part A **68** (2005) 1–19.

Liebau, F. (1985): Structural Chemistry of Silicates: Structure, Bonding and Classification. Springer, Berlin.

Merlino, S.; Bonaccorsi, E.; Grabezhev, A. I.; Zadov, A. E.; Pertsev, N. N.; Chukanov, N. V.: Fukalite: An example of an OD structure with two-dimensional disorder. Am. Mineral. **94** (2009) 323–333.

Mizota, T.; Komatsu, M.; Chihara, K.: A refinement of the crystal structure of ohmilite, $Sr_3(Ti,Fe^{3+})(O,OH)(Si_2O_6)_2 \cdot 2–3\ H_2O$. Am. Mineral. **68** (1983) 811–817.

Moore, P. B.: A novel octahedral framework structure: gageite. Am. Mineral. **54** (1969) 1005–1017.

Moore, P. B.; Araki, T.: Pinakiolite, $Mg_2Mn^{3+}O_2[BO_3]$; warwickite, $Mg(Mg_{0.5}Ti_{0.5})O[BO_3]$; wightmanite, $Mg_5(O)(OH)_5[BO_3] \cdot nH_2O$: crystal chemistry of complex 3 Å wallpaper structures. Am. Mineral. **59** (1974) 985–1004.

Nespolo, M.; Ferraris, G.: Effects of the stacking faults on the calculated electron density of mica polytypes – Ďurovič effect. Eur. J. Mineral. **13** (2001) 1035–1045.

Phillips, A. H.: Gageite, a new mineral from Franklin, New Jersey. Am. J. of Science **30** (1910) 283–284.

Plaisier, J. R.; Ijdo, D. J. W.; de Mello Denegs, C.; Blasse, G.: Structure and luminescence of barium uranium disilicate ($BaUO_2Si_2O_6$). Chem. Mater. **7** (1995) 738–743.

Rastvetaeva, R. K.; Pushcharovskii, D. Yu.; Konev, A. A.; Evsyunin, V. G.: Crystal structure of K-containing batisite. Crystallogr. Rep. **42** (1997) 770–773.

Sheldrick, G. M.: A short history of *SHELX*. Acta Crystallogr. **A64** (2008) 112–122.

Takéuchi, Y.; Joswig, W.: The structure of haradaite and a note on the Si–O bond lenghts in silicates. Mineral. J. (Japan) **5** (1967) 98–123.